Renewable Energy 221 (2024) 119822

Contents lists available at ScienceDirect

Renewable Energy

journal homepage: www.elsevier.com/locate/renene

Sizing and scheduling optimisation method for off-grid battery photovoltaic irrigation networks

M.A. Pardo [a,*], F.J. Navarro-González [b]

[a] Department of Civil Engineering, University of Alicante, 03690, Alicante, Spain
[b] Department of Applied Mathematics, University of Alicante, 03690, Alicante, Spain

ARTICLE INFO

Keywords:
Pressurized irrigation networks
Batteries
Energy consumption

ABSTRACT

An algorithm to optimise the number of solar panels and battery size to meet the water demands of an installation has been developed. The algorithm adjusts for seasonal changes in energy use and production in a pressurized irrigation network and production in an off-grid solar panel system. By using this algorithm, we aim to create an efficient and sustainable irrigation system by reducing the infrastructure and reliance on the power grid. This method can enhance irrigation systems in far-off regions, strengthen their endurance, and promote sustainable energy in farming and water administration.

1. Introduction

Irrigation plays a significant role in the water consumption of Southern European countries, amounting to 70 % of the total [1,2]. The World Bank and FAO also affirm these statistics [3]. Using less water for irrigation helps the environment by reducing energy use and GHG emissions. To achieve a reduction in emissions, the European Union (EU) wants to reduce total energy demand by 20 %. The EU encourages using renewable energies like wind and solar, which have grown faster than other industries in the last decade. The Paris Agreement and the EU Green Deal [4] encourage the use of renewable energy. Both documents underline the progress of photovoltaics in the EU. The European Union takes on the legally binding target of reaching 27 % of its energy consumption from renewable energy sources by 2030 [5]. In Spain, the government published a law (6 April, RD 244/2019) establishing new regulations for photovoltaic energy. Photovoltaic solar panel costs fell by 70 % in the last decade, helping the growth of the industry [6]. Another important factor is the high price of electricity. Energy costs in August 2022 were the highest in history, averaging 307.8 €/MWh. Likewise, the day with the most expensive average electricity price ever seen in Spain was March 8, 2022, with 544.98 €/MWh. The high price of energy caused inflation to reach a historical maximum of 10.8 % in July 2022 and the Consumer Price Index stood at 5.7 % in December 2022 [7].

Solar energy is popular in irrigation because it can help with energy and environmental issues [8,9]. Studies have investigated using solar power for irrigation systems [10–12]. The shift towards solar-powered irrigation setups offers promising advantages, notably in regions with limited access to traditional power grids. Using solar-powered pumping networks can save energy and sustain water supply for farmers and managers [13,14]. This method can improve irrigation by making it eco-friendly, which can help save resources and reduce the impact of climate change.

In water-pressurized networks, compensation tanks serve a dual purpose by providing a means for storing both water and energy [15]. The tanks keep the hydraulic pressure steady to provide a dependable water supply. This solution stores water for irrigation when there is no sunlight or energy available, being called a virtual battery [16]. Numerous authors compared energy storage in batteries or tanks (off-grid) [17,18]. There isn't a single solution because several factors affect the outcome. A study in Alicante Province found that using a tank is the best option for a pressurized water network [19]. where the tank alternative resulted as the best choice. This option can limit if there is no compensation tank, or the terrain is too flat for installation. Finally, it appears a third strategy that involves the pumping system can be on-grid. So, this extra energy can be injected into the grid to get money from the electricity grid company.

By integrating reverse osmosis desalination and pump storage systems with wind and photovoltaic energy, we address water and energy challenges holistically [20]. The study also put forth a range of intelligent strategies to enhance the incorporation of renewable energy sources across multiple sectors [21]. This includes approaches like price

* Corresponding author.
E-mail address: mpardo@ua.es (M.A. Pardo).

https://doi.org/10.1016/j.renene.2023.119822
Received 7 September 2023; Received in revised form 14 November 2023; Accepted 14 December 2023
Available online 18 December 2023

forecasting and scheduling in the market to reduce costs and enhance the local market operator's flexibility [22], and boosting the adoption of renewable energy sources and capitalising on synergistic opportunities whenever feasible [23]. Photovoltaic systems are increasingly being utilised for desalination processes, reducing the values of unitary investment costs are 0.67–0.76 USD/m^3 [24], or by 20 % [25].

A variety of research endeavours examined distinct aspects within the realm of solar-powered irrigation systems. One group focused on determining the optimal system size [26], while a separate set delved into the realm of autonomous irrigation scheduling [27]. Some approaches [28] found that certain systems can use up to 75 % of the energy from PV modules under certain irrigation conditions. Pumping PV irrigation works better than doing things separately because it uses less energy and allows for more irrigation time [14]. Finally, other methods improved renewable energy use [29] and lowered electricity costs [30].

Efficient water infrastructure requires managers to synchronise energy usage and production. In pressurized water distribution networks, managers can adjust water usage according to energy production. Previous research [31] successfully solved synchronisation and achieved a coordinated system. Irrigation managers can choose schedules that match both crop water needs and energy from PV panels. Using this approach can lead to sustainable water and energy management in agriculture.

Batteries are important for using renewable energy at home. They give flexibility and let you use the energy you make [32]. Lithium-ion batteries are the best option for storing wind or solar energy power [33,34], and some studies help choose the best battery technology [35]. The proper size of a battery system plays an important role in the total minimisation of the system's cost during its lifetime [36]. Researchers in Egypt [37] designed a solar system for irrigation. They found the best combination of solar panels and batteries based on the weather in the test area. The ideal configuration of a solar-powered sprinkler system is determined using data from a typical sunny day in the test area. To get the best results, we need to choose the right PV module and battery combination [26].

This study aims to create an algorithm that optimises the size of solar panels and batteries to meet the water needs of a pressurized irrigation system. The algorithm is made for irrigation networks that use solar panels. The study compared the optimisation algorithm results for the same installation in December and July. This approach balances resource use and efficiency to make irrigation sustainable and affordable. A case study was presented at the University of Alicante gardens on daily energy consumption using a specific flow distribution.

The study is limited to off-grid pumps and solar panels used to power pressurized irrigation systems. To analyse the system, practitioners need data on pump characteristics, water usage per unit, and the number of pumps running together. To compare various scenarios, the study uses the same amount of water demanded by the crops. Only crop water needs to determine the amount of water volume, not how energy is made. To install it, you need to know which PV solar panel to use and some physical characteristics, such as latitude and longitude.

This study delves deeper into the correlation between solar energy, its direct use in pumping machinery, and storage. Thus, it is crucial to address the irrigation needs of the crops while sizing the installation and the battery appropriately. Clearly, the goal is to minimise the reliance on such installations and enhance self-sufficiency through local solar energy. As a result, there is a strong impetus to develop off-grid strategies for several compelling motives. These include cost stability, reducing emissions, and optimising investments for off-grid operations. This research aims to overcome barriers to adding PV systems to Pressurized Irrigation Networks by involving PV system operators and stakeholders in the energy management process.

The contributions of the paper can be summarised as.

- First, this study introduces an optimisation algorithm aimed at scheduling water supply in irrigation networks. The algorithm achieves this by dynamically adjusting the energy demanded by irrigation pumps to minimise the energy stored in batteries. This energy stored in batteries is calculated as the difference between the energy produced by solar photovoltaic panels and the energy consumed in the pumps.
- Furthermore, the proposed algorithm reduces the size of PV panels and batteries needed by transforming a pumping system to function as a standalone system, recognising the energy-intensive nature of managing irrigation systems. This approach ensures that the installation is not oversized, optimising energy utilisation. As the batteries are considered in this approach, the solar power system is also reduced.
- Lastly, the proposed algorithm shows computational efficiency and can be universally applied to any location. It adeptly addresses the seasonal variation in irradiance and water demand from crops, making it a versatile and effective solution for managing irrigation systems.

This is a useful tool for managers and decision-makers who want to make their irrigation system autonomous using solar panels and batteries. The paper is structured as follows. Section 2.1 explains the method for calculating PV module energy production, while section 2.2 delves into the power consumption aspects of water-pumping devices. Section 2.3 segment expounds upon critical points for minimising battery requirements, and section 2.4 introduces the algorithm alongside its pseudocode. A real-life case study is presented in section 3, detailing energy consumption and PV production data under sections 3.1 and 3.2 respectively. Section 4 highlights the results and section 5 analyses the results and suggests future research. Section 6 presents the conclusions.

2. Materials and method

2.1. The energy generated by solar panels

In this work, we will consider an installation composed of n_s solar panels, which, for simplicity, are assumed to be of the same type with identical characteristics. Letting $P^1_{gen}(t)$ be the function that represents the generated power (irradiance) at each moment by one of these panels, the total power generated by the set of panels (n_s) is given by $P^{n_s}_{gen}(t) = n_s \bullet P^1_{gen}(t)$. The function $P^1_{gen}(t)$ is influenced by the panels as well as the geographical and climatic conditions specific to the installation's location.

Determining the irradiance produced by a panel is a complex problem for which there is abundant literature [38–40]. The problem can be decomposed into different parts, depending on the considerations incorporated into it. The 'clear sky model' assumes no factors like clouds that could decrease radiation on the panel. Thus, the direct irradiance P_0 on a ground-level panel can be modelled as a function of the solar zenith angle using equation (1):

$$P_0 = P_{0N} \bullet cos(\theta_s) \tag{1}$$

Being P_{0N} the irradiance on a normal surface, θ_s the solar zenith angle, related to the location latitude (φ), the solar declination (δ) and the solar hour angle (ω) measured from the local meridian to the sun's position at each moment through equation (2):

$$cos(\theta_s) = sin(\varphi) \bullet sin(\delta) + cos(\varphi) \bullet cos(\delta) \bullet cos(\omega) \tag{2}$$

The solar hour angle can be replaced by the reduced time as $t = \frac{12}{\pi} \bullet \omega$, taking values over the interval $[-12, 12]$, with $t = 0$ corresponding to noon.

If the solar panel is tilted at an angle β towards noon, the sun's incidence can be determined by equation (3):

$$cos(i) = sin(\Phi - \beta) \bullet sin(\delta) + c's(\Phi - \beta) \bullet cos(\delta) \bullet cos(\omega) \quad (3)$$

Introducing this expression into equation (1) allows us to obtain the power generated by the panel through equation (4):

$$P^{1}_{gen}(t) = A + B \bullet cos\left(\frac{\pi}{12} \bullet t\right) \quad (4)$$

The model can be expanded to include atmospheric attenuation and its impact on various wavelengths based on the air layer thickness. Similarly, there are other components, such as diffuse radiation (which comes from atmospheric scattering in various directions) and albedo (the portion of radiation reflected because ultimately impacts the solar panel from different directions).

This work focuses on equation (4), estimating values for parameters A and B by comparing measured irradiance in July and December. These two parameters were calculated using Eqs. (5) and (6).

$$A = \frac{\pi}{24} \frac{E^{1}_{panel} \bullet cos(\omega_s)}{sin(\omega_s) - \omega_s \bullet cos(\omega_s)} \quad (5)$$

$$B = \frac{\pi}{24} \frac{E^{1}_{panel}}{sin(\omega_s) - \omega_s \bullet cos(\omega_s)} \quad (6)$$

2.2. Pump operation optimisation

From another perspective, the water flow will be supplied by a set of pumps, which, for the sake of problem simplification, will be considered of the same type. These pumps will be characterized by their performance curve $P = F(Q)$. In general, when there are i pumps working together, the effective power used to deliver a flow Q is determined by the function denoted by $P = F_i(Q)$. An example can be seen in Fig. 1 [28] where we examined a scenario involving the case of three pumps connected in parallel "EVM 32 2-0F5/4.0".

Given a flow rate Q = 5 l/s (Fig. 3 [28]), illustrates the various possibilities to meet this demand, depending on the number of pumps involved. These results can invert the curves $P = F_i(Q)$, determining the maximum available flow Q for each power $Q = F_*(P) = \max_i F_i^{-1}(P)$ (see Fig. 4).

The number of pumps in operation is determined by the expression of $F_*(P)$, and we can calculate it using the step function $i = \left[\frac{F_*(P)}{Q_{max}}\right] + 1$, where [x] represents the floor function. Therefore, there is no need to include any index sign in the inverse function $F_*(P)$. The efficiency of each operational combination *(P, Q)* corresponds to the slope of the straight line connecting the origin to the point *(P, Q)*, $\eta = \frac{F_*(P)}{P}$. When i pumps are operating in parallel, the optimal value of η corresponds to

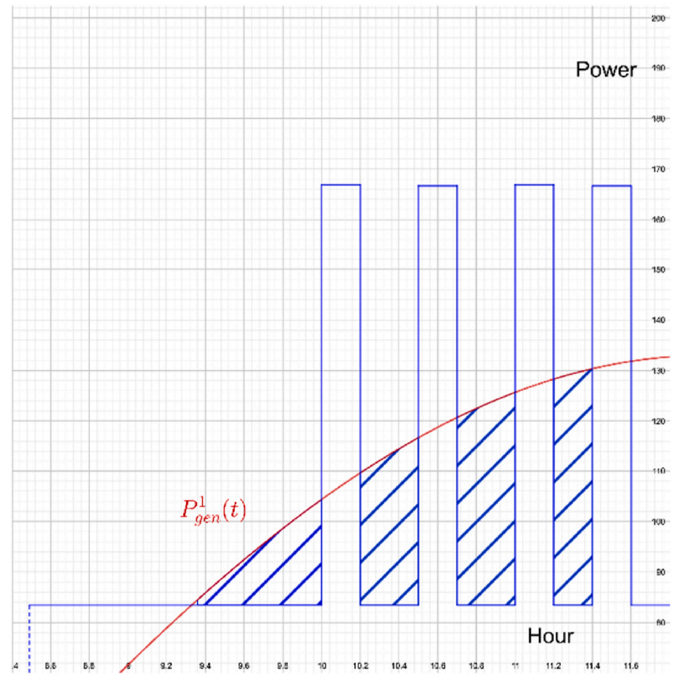

Fig. 2. Solution based on micro-intervals.

Algorithm 1 Optimum installation size and candidate paterns of power consumption

Input:
Q_*: Optimum flux served by the pump (see Figure3),
P_*: Optimum power corresponding to $P_* = F_1(Q_*)$,
V_{day}: Total daily volume of water,
E^1_{panel}: Total daily energy generated by the generic solar panel ,
$P^1_{panel,max}$: Maximum power generated by the panel
Output:
N_{opt}: Number of pannels
K: Candidate configurations (max. number of pumps working)
procedure OPTIMIZEINSTALLATIONSIZE
$\eta \leftarrow Q_*/P_*$
$E_{pumps} \leftarrow V_{day}/\eta$
$N_{opt} \leftarrow V_{day}/(\eta \cdot E^1_{panel})$
$K \leftarrow Ceil(P^1_{panel,max}/P_*)$
return N_{opt}

Fig. 3. Optimum installation size algorithm.

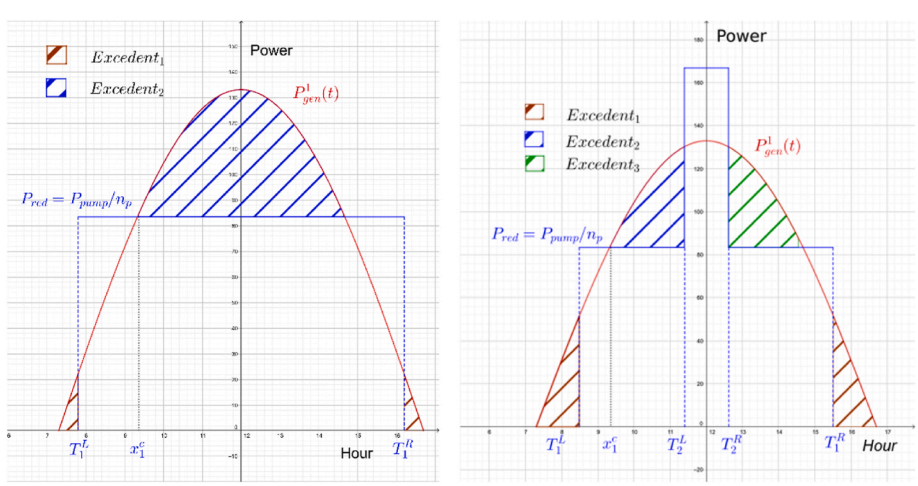

Fig. 1. Graphical representation of the problem: (a) with one pump operating, (b) with two pumps operating.

$\eta_i = \frac{i \bullet Q_{max}}{F_i(i \bullet Q_{max})}$. With a system of homogeneous pumps, the above expression simplifies since the points are integer multiples of $(F_1(Q_{max}), Q_{max})$.

2.3. Solar panel-battery system size optimisation

For resolving the optimal system configuration planning problem, its general aspect can be considered, as shown in Fig. 3. As introduced in the previous section, $P^1_{gen}(t)$ corresponds to the irradiance curve for a standard panel, while $P_{red} = \frac{P_{pumps}}{n_s}$ is the proportional part of the constant power consumed by a pump during its operation that must be supplied by a single panel. The critical points x^c_1, T^L_i and T^R_i are the points of intersection between the reduced power curve and the start and stop intervals with i pumps working, respectively.

The work plan determines which irrigation points and pumps are connected or disconnected in the network being studied. Each possible work plan involves a certain energy consumption associated with the pumps that supply the water required by the system. First, the balance between the energy consumed by a specific work plan and the energy generated by the solar panel installation can be considered.

The consumed energy is the energy generated by the irradiance incident on the set of panels, and it is obtained as follows (Equation (7)):

$$\sum_j \sum_i^{n_p} \pi_i \bullet \left(\delta^R_j - \delta^L_j\right) \bullet T^j_i = n_s \bullet E^{gen}_1, \tag{7}$$

where n_p is the number of pumps in operation, n_s represents the number of solar panels, E^{gen}_1 is the energy generated in a day by a single panel, $(\delta^R_j - \delta^L_j) \bullet T^j_i$ accounts for the operating time of the combination of i pumps, and π_i is the optimal operating power obtained from F_i.

On the other hand, the water flow delivered during the complete operating period of the pumps must equal the total volume required by the system, according to equation (8):

$$\sum_j \sum_i^{n_p} Q_i \bullet \left(\delta^R_j - \delta^L_j\right) \bullet T^j_i = V_{TOT}, \tag{8}$$

where Q_i is the flow obtained under the optimal operating conditions for i-connected pumps. These conditions were introduced in Figs. 1–3 and imply a relationship between the flow and the operating power, given by $Q_i = \eta_i \bullet \pi_i$. By incorporating this expression into equation (8) and introducing the reduced power $P^i_{red} = \frac{\pi_i}{n_s}$, the problem conditions can be written as follows (equation (9)):

$$\begin{aligned} &\sum_j \sum_i^{n_p} P^i_{red} \bullet \left(\delta^R_j - \delta^L_j\right) \bullet T^j_i = E^{gen}_1 \\ &\sum_j \sum_i^{n_p} \eta_i \bullet P^i_{red} \bullet \left(\delta^R_j - \delta^L_j\right) \bullet T^j_i = \frac{V_{TOT}}{n_s} \end{aligned} \tag{9}$$

Where the pumps are identical, the problem of determining the optimal n_s is simplified since $\eta_1 = \cdots = \eta_{n_p} = \eta$, which leads to equations (10) and (11):

$$\eta \bullet E^{gen}_1 = \frac{V_{TOT}}{n_s}, \tag{10}$$

And it results in:

$$n^*_s = \frac{V_{TOT}}{\eta \bullet E^{gen}_1} \tag{11}$$

This number is the minimum number of panels required to meet the pumping system's needs during the supply of the required volume. The power comes from the solar panels and the stored battery energy (equation (12)).

$$P(t) = n^*_s \bullet P^1_{gen}(t) + P_{saved}(t) \tag{12}$$

Equation (13) defines an objective function to minimise energy storage needs during the process.

$$\Phi(P(t)) = \max_t P_{saved}(t) = \max_t \left(P(t) - n^*_s \bullet P^1_{gen}(t)\right) \tag{13}$$

The function $\mathrm{P_{optimal}}(t)$ that minimises $\Phi(P(t))$ is called the energy consumption pattern and induces a corresponding pattern in the target flow through the equation

$$Q_{optimal}(t) = F_*\left(P_{optimal}(t)\right) \tag{14}$$

Although micro-intervals can solve the issue, frequent pump connections cause pressure instability, making them not practical. This solution involves using brief intervals where energy is stored and immediately spent in the next interval, as seen in Fig. 2.

To avoid frequently connecting/disconnecting pumps, we will examine solutions based on Fig. 1. The optimisation of the battery size associated with the system is resolved by considering different scenarios where several pumps are used between $n_p = 1$ and $n_p = \left[\frac{\mathrm{P^1_{gen}}(12)}{P^1_{red}}\right] + 1$. Once the optimal pattern for i pumps has been calculated, the surplus energies in each excess period of this optimal pattern are computed, determining the minimum storage capacity required for the batteries with the operating pattern of i+1 pumps. The goal is to minimise stored energy while still having enough for future deficits. To make these modifications, we reduce the operating time of some pumps and give more time to others. This process continues until any reorganisation results in an increase in the required storage in any of the excess periods.

2.4. Optimal irrigation scheduling

In the final stage of optimisation, we plan the flows for each irrigation point to synchronise pump operation with optimal values. Using an additional objective function (equation (15)), we can solve the problem of calculating the difference between the optimal flow and the irrigation plan flow.

$$\Phi(\Pi) = \frac{1}{T} \sum_{k=1}^{T} [\mathrm{Q}(t_k) - \pi(t_k)]^2, \tag{15}$$

where $\pi(t_k)$ is the flow allocated in the interval k, which at the beginning of the algorithm would be initialised to 0 for all t_k, and $\mathrm{Q}(t_k)$ is the available flow in t_k.

Considering an alternative plan Π' that differs from the first one in the modification $\pi'(t_i) = \pi(t_i) + \Lambda$, for arbitrary i, the change in the objective function can be obtained from equation (15), being the objective function as equation (16).

$$\Phi(\Pi') = \Phi(\Pi) + \Lambda \bullet [\Lambda - 2 \bullet (\mathrm{Q}(t_i) - \pi(t_i))], \tag{16}$$

Since the aim is the minimisation of the functional $\Phi(\Pi)$ and Λ is a fixed value, the maximum decrement will be obtained by taking the largest of the differences in $\mathrm{Q}(t_i) - \pi(t_i)$ within the current program, provided that the conditions $\mathrm{Q}(t_i) - \pi(t_i) > 0$ and $\Lambda - 2 \bullet (\mathrm{Q}(t_i) - \pi(t_i)) < 0$ are satisfied.

Then, the steps to solve the problem can be resumed at the following points.

1 Given the demand for water for the installation (V_{tot}), the characteristics of the pumping system (through the values of Q_{max} and $F_1(Q_{max})$) and the solar panel power curves the size of the solar installation is determined using equation (9). Once the total power curve of the solar installation is available, $P^{tot}_{gen}(t) = n^*_s \bullet P^1_{gen}(t)$, the pattern of power consumption is calculated using Algorithm 1. This algorithm also obtains the needs of energy saving for the system. The

first part of the algorithm determines the number of solar panels required to satisfy the irrigation needs of the installation under consideration. The pseudocode can be seen in Fig. 3:

2 Using the function $Q = F_*(P)$, the pattern of an objective flow $Q^*(t)$ is obtained (see Algorithm 2; Fig. 4). The second task determines the optimal approach for arranging pump connection, aiming to minimise storage needs for auxiliary battery systems, while ensuring we can meet all energy periods of energy deficit according to the selected planning (see Fig. 6):

To obtain this optimum, it is necessary to use the auxiliary functions CreateLeftAlternative and CreateRightAlternative, which construct alternative consumption plans to the one selected at a time, so that the best among we choose them at each iteration (Figs. 5 and 6).

3 From the function $Q^*(t)$, the optimal irrigation plan is determined to minimise the difference between the flow served at each instant and the pattern $Q^*(t)$, as can be seen in Algorithm 3. The concluding phase of the optimisation process involves establishing the ideal irrigation schedule, encompassing the arrangement of connections and disconnections at each PIN. The outcome aims to minimise the overall required volume by continuously minimising the disparity between the flow achievable through pumps powered by solar panels

```
Algorithm 2 Optimization of pumps operation
Input:
  N: Total number of slides,
  N_output: Number of slides with operating pumps,
  P: Nominal pump power,
  Δt: Size of time slide (in hours)
Output:
  Output_1, ··· , Output_N: Power consumption by slide
  procedure OptimizePumpsScheduling
    χ ← (N − N_output)/2
    /*Init with 1 pump scheduling*/
    for i in 0, ··· , N do
      if ibetween(χ, N_output + χ) then
        Output_i ← P · Δt
        Saved_i ← Input_i − Output_i
        Net_i ← Saved_i
        if i ≠ 0 then
          Net_i = Net_i + Net_{i−1}
    Fit_best ← max_{i=1,···,N} (Net_i)
    L_left ← [χ ; N/2] ; L_right ← [χ + N_output ; N/2]
    flag ← True
    /*Optimizing with 2 pumps scheduling*/
    while flag do
      OutL, SavedL, NetL ← CreateLeftAlternative(Output, L_left)
      OutR, SavedR, NetR ← CreateRightAlternative(Output, R_left)
      /*Updating with the best alternative*/
      if max_{i=1,···,N} (NetL_i)) < Fit_best then
        Output ← OutL
        Saved ← Input − OutL
        Net ← NetL
        Fit_best ← max_{i=1,···,N} (NetL_i))
        L_left ← L_left + [1 ; −1]
      else if max_{i=1,···,N} (NetR_i)) < Fit_best then
        Output ← OutR
        Saved ← Input − OutR
        Net ← NetR
        Fit_best ← max_{i=1,···,N} (NetR_i))
        R_left ← R_left + [−1 ; 1]
      else                          ▷ If there is no improvement, it will leave
        flag ← False
    return Output_1, ··· , Output_N
```

Fig. 4. Optimum pump connection scheduling.

```
Algorithm 2 Optimization of pumps operation
Input:
  N: Total number of slides,
  Output: Power consumption by slide,
  P: Nominal pump power,
  Δt: Size of time slide (in hours)
  L_left: Left starting slides (one and two pumps)
Output:
  OutL: Alternative power consumption by slide
  SavedL: Alternative power consumption by slide
  NetL: Alternative power consumption by slide
  procedure CreateLeftAlternative
    OutL_{L^1_left} ← Output_{L^1_left} − P · Δt
    OutL_{L^2_left} ← Output_{L^2_left} + P · Δt
    SavedL_{L^1_left} ← Output_{L^1_left} + P · Δt
    SavedL_{L^2_left} ← Output_{L^2_left} − P · Δt
    OutR_{L^1_right} ← Output_{L^1_right} − P · Δt
    for i in 0, ··· , N do
      NetL_i ← SavedL_i
      if i ≠ 0 then
        NetL_i = NetL_i + NetL_{i−1}
    return OutL, SavedL, NetL
```

Fig. 5. Auxiliar function CreateLeftAlternative.

```
Algorithm 2 Optimization of pumps operation
Input:
  N: Total number of slides,
  Output: Power consumption by slide,
  P: Nominal pump power,
  Δt: Size of time slide (in hours)
  L_right: Right starting slides (one and two pumps)
Output:
  OutR: Alternative power consumption by slide
  SavedR: Alternative power consumption by slide
  NetR: Alternative power consumption by slide
  procedure CreateRightAlternative
    OutR_{L^1_right} ← Output_{L^1_right} − P · Δt
    OutR_{L^2_right} ← Output_{L^2_right} + P · Δt
    SavedR_{L^1_right} ← Output_{L^1_right} + P · Δt
    SavedR_{L^2_right} ← Output_{L^2_right} − P · Δt
    for i in 0, ··· , N do
      NetR_i ← SavedR_i
      if i ≠ 0 then
        NetR_i = NetR_i + NetR_{i−1}
    return OutR, SavedR, NetR
```

Fig. 6. Auxiliary function CreateRightAlternative.

and the battery system, and the cumulative consumption at each PIN. The associated pseudo-code is depicted in Fig. 7:

3. Case study

3.1. Energy consumption data

The PIN (Pressurized Irrigation Network) of the University of Alicante (38°23′4.06″ N, 0°30′44.06″ W), in south-eastern Spain, is analysed as a case study of Spain (Fig. 8). The irrigation area of this garden has expanded over time, and the gardeners have introduced new species to the grass meadow, such as Festuca arundinacea and Poa annua. We subdivided the plot into hydro-zones, following the landscape coefficient method, which considers water requirements and crop evapotranspiration values. During the months with the highest water demand, the total water requirements range from 1.7 to 3.9 L per square millimeter per day, similar to the water consumption in the least and most exposed areas of the garden. A comprehensive description study can be found in the work by Ref. [28]. This garden has 891 pipes made of polyvinyl chloride and fibre cement. The irrigated area covers 0.67 km^2 and we set the roughness coefficients to 100. The total length of the pipes is 23 km, and their diameters are below 200 mm. There are 160

Algorithm 3 PIN Water delivery scheduling

Input:
N_{output}: Number of slides with operating pumps,
$Q^{(1)}, .., Q^{(N_{output})}$: Available flow on each slide with operating pumps,
ε: Tolerance
Output:
$s^{(1)}, .., s^{(N_{output})}$: Vector of scheduling slides,
$V^{(1)}, .., V^{(N_{output})}$: Injected volume by slide
procedure OPTIMIZESCHEDULING
  /*Initialize variables*/
  for $i \leftarrow 1, N_{output}$ **do**
    $s^{(i)} \leftarrow \emptyset$
    $V^{(i)} \leftarrow 0$
  /*Read network data*/
  Read devices: $(d_1, .., d_{N_d})$
  Read device flows: $(\Phi_1, .., \Phi_{N_d})$
  $i \leftarrow 1$
  while $\sum_{m=1}^{N_{output}} Q^{(m)} < \varepsilon$ **do**
    $device \leftarrow d_i$
    $k \leftarrow \{j \mid V^{(j)} = max(Q^{(m)}, m = 1..N_{output})\}$
    $s^{(k)} \leftarrow s^{(k)} + d_i$
    $V^{(k)} \leftarrow V^{(k)} + \Phi_i$
    $Q^{(k)} \leftarrow Q^{(k)} - \Phi_i$
  return $s^{(1)}, .., s^{(P)}, V^{(1)}, .., V^{(P)}$

Fig. 7. Optimisation of PIN scheduling.

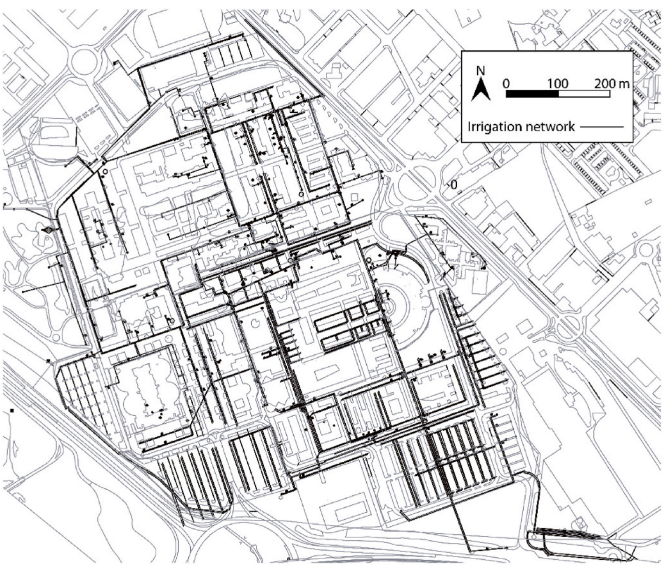

Fig. 8. The university of alicante-irrigation system.

consumption nodes equipped with valves to control the water delivery to each node. The water distribution to these consumption nodes must maintain a pressure above the threshold value of $\left(\frac{p}{\gamma}\right)_{th} = 25$ m.w.c.

We provide water to the pressurized irrigation network through the reservoir, which is near the university. However, it is possible to draw water from the drinking water supply network in San Vicente del Raspeig for irrigation as well. The irrigation system comprises a set of three identical pumps working in parallel ("EVM 32 2-0F5/4.0" of the "Ebara" company). The pump curve is $H = -0.2163Q^2 + 0.3509Q + 44.713$. Based on the nominal values of the pumps, we find that the optimal working power is $P = 3.337\ kW$, which corresponds to a flow rate of $Q = 15\ l/s$. The pump can start anytime but must run for at least 15 min for the simulation. We can do only three starts per hour because of mechanical limitations. This prevents damage to the equipment and excessive power consumption.

3.2. Energy production data

To determine the energy produced by a single PV panel, we calculate irradiance from the Duffie and Beckman equations [41]. The parameters required to calculate the hourly energy produced by PV arrays were described in Ref. [28]. Under the conditions of equal sunset hour angle (ω_s) and total day-generated energy ($E^1_{panel,jul} = 1990.71\ W \bullet h/day$ and $E^1_{panel,dec} = 779.17\ W \bullet \frac{h}{day}$), the irradiance equation results in a Kasten–Czeplak model, obtaining the parameters A and B of equation (4). The energy required by the pumps to serve the demanded volume of water $V_{week} = 3078.2\ m^3$, or equivalently, the daily amount $V_{day} = 493.74\ m^3$ can be calculated by considering equation (17).

$$E_{pumps} = P_{pumps} \bullet T = \frac{Q}{\eta} \bullet T = \frac{V_{day}}{\eta} \quad (17)$$

We consider two different scenarios for December and July, denoted by the subscripts "dec" and "jul" in the respective variables. By comp"rin" the "upp"ied energy and the energy required for the pumps, it follows equation (18):

$$n_s = \frac{V_{day}}{\eta \bullet E^1_{panel}} \quad (18)$$

3.3. Results in December

First, in December, the energy obtained in a single module is equal to $E^1_{panel,dec} = 779.17\ Wh$, the number of solar modules is equal to $n_s = \frac{V_{day}}{\lambda \bullet E^1_{panel}} = 39.2 \sim 40$. The value of this reduced power is $P_{red,dec} = \frac{P_{pumps}}{n_s} = 83.425\ W$. When there is only one pump in operation, the required operating time to provide the total volume of water is given by equation (7)), resulting in $T_1^L = 7.316\ h$ and $T_1^R = 16.66\ h$. This means that the pump would be turned on at 7:19:48 and turned off at 16:40:12 (Fig. 9). The energy stored during the period between $x_1^c = 9{:}46$ and 14:54 (central zone) corresponds to P^1_{gen} (t) = 157.05 Wh (Fig. 9).

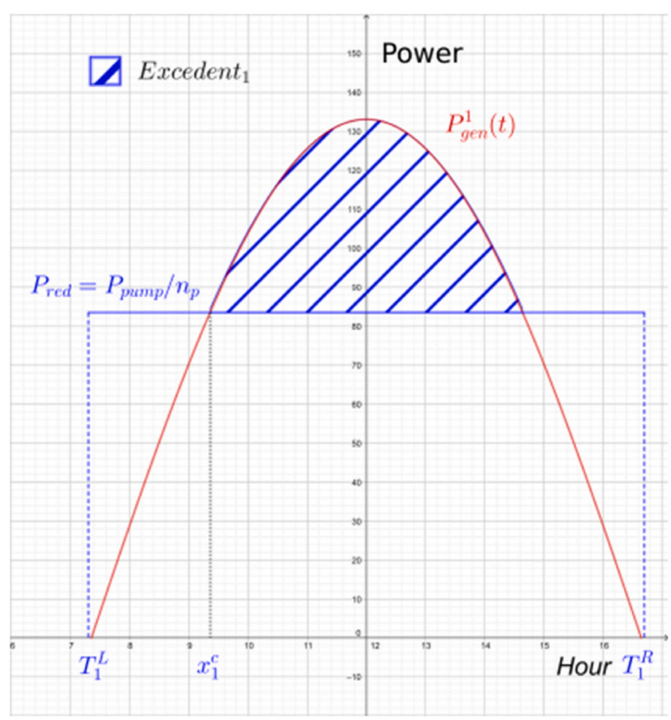

Fig. 9. Power generated and consumed for the December scenario with one pump in operation.

By increasing the number of pumps to two, we create two new storage zones visible in in Fig. 1b, and we decrease the required capacity. Each surplus period should store enough energy to cover the following deficit period. Follow these steps to get the numerical solution: refer to Fig. 10 and transfer consumption to the central zone with two pumps. The optimum is the point where any additional modification results in an increase in the battery's capacity system. The best solution is when each excess period stores enough energy to cover a deficit period. The result is depicted in Fig. 10 and the energy stored in Fig. 11, while the numerical results are shown in Table 1.

Table 1 summarises the various configurations studied.

In December, it's important to optimise irrigation points to avoid excess flow depicted in Fig. 12. This surplus represents the volume of water that the system could deliver compared to what is required. As observed, this excess is nearly constant throughout all instances but is shifted away from the desirable target value of zero.

In conclusion, we can effectively address the irrigation scheduling problem by employing the mean square error minimisation method outlined in Ref. [42] for the function, resulting in equation (19) specifically tailored for December.

$$f_{Dec}(t)=P_{red,Dec}\bullet\left\{2\bullet H\left(T^{R}_{2,Dec}\right)+H\left(T^{R}_{1,Dec}\right)-H\left(T^{L}_{1,Dec}\right)-2\bullet H\left(T^{L}_{2,Dec}\right)\right\} \quad (19)$$

Being $H(x)$ the Heaviside step function.

3.4. Results in July

The energy produced in a single module is equal to $E^{1}_{panel,jul}=1990.71\ Wh$, the number of solar modules is equal to $n_s=\frac{V_{day}}{\lambda\bullet E^{1}_{panel}}=15.33\sim 16$. The value of this reduced power is $P_{red,dec}=\frac{P_{pumps}}{n_s}=208.56\ W$. Fig. 13 shows the corresponding powers and critical points ($T^{L}_{1}=7.216h$; $T^{R}_{1}=16,76h$):

The stored energies in the first and second surplus periods are 174.62 *Wh* and 121.82 *Wh* respectively. Adding another pump means increasing the size of surplus zone 1 and the batteries. Thus, in July, the optimal operating profile corresponds to connecting only one pump. The results can be seen in Table 2

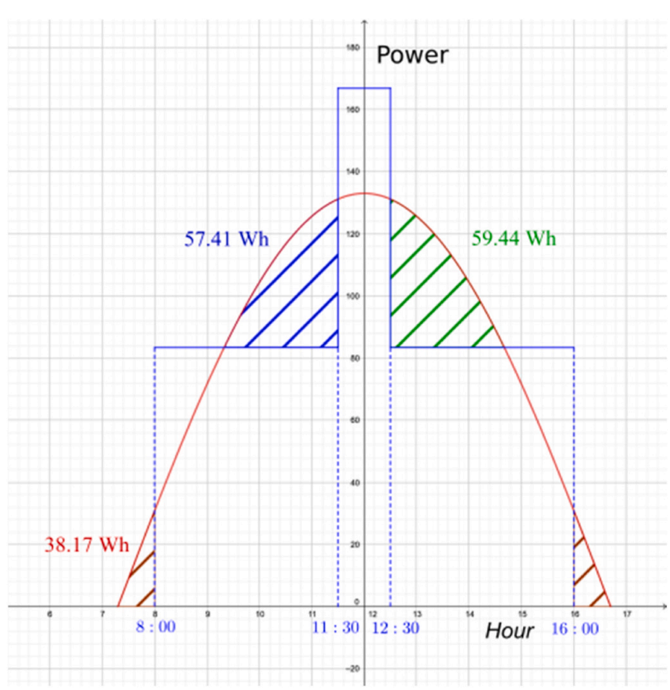

Fig. 10. Power generated and consumed in the optimal scenario for December.

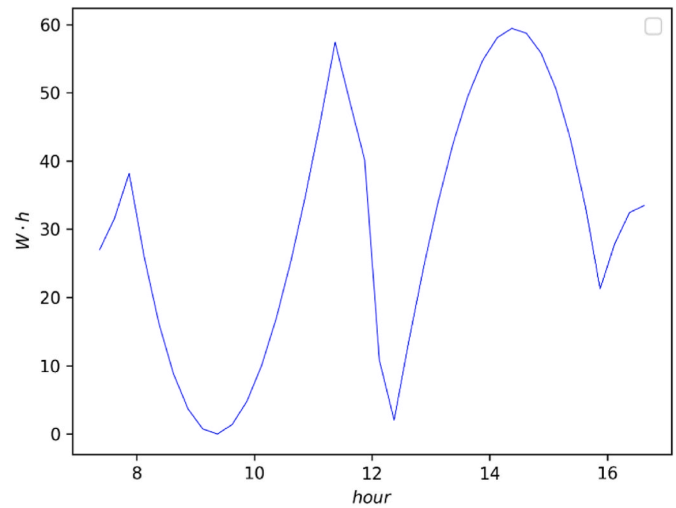

Fig. 11. Energy stored for the hour of the day.

Table 1
Numerical results for the key variables corresponding to December.

One pump operating			
$T=\frac{V_{day}}{\lambda\bullet P_{red}}$	9.34 h	T^{L}_{1} / T^{R}_{1}	7:19:48/16:40:12
Period	Energy stored	Energy consumed	Balance
7.33 – 9.46	95.94 *Wh*	177.70 *Wh*	– 81.76 *Wh*
9.46 – 14.54	587.29 *Wh*	423.80 *Wh*	163.49 *Wh*
14.54 – 16.67	95.94 *Wh*	177.70 *Wh*	– 81.76 *Wh*
Two pumps operating			
T^{L}_{1} / T^{R}_{1}	8.37/15.63	T^{L}_{2} / T^{R}_{2}	11.39/12.61
Period	Energy stored	Energy consumed	Balance
7.33 – 8.37	26.16 *Wh*	0 *Wh*	26.16 *Wh*
8.37 – 9.46	69.78 *Wh*	91.27 *Wh*	– 21.48 *Wh*
9.46 – 11.39	213.22 *Wh*	161.01 *Wh*	– 81.76 *Wh*
11.39 – 12.61	160.85 *Wh*	203.56 *Wh*	– 81.76 *Wh*
12.61 – 14.54	213.22 *Wh*	161.01 *Wh*	157.05 *Wh*
14.54 – 15.63	69.78 *Wh*	91.27 *Wh*	– 81.76 *Wh*
15.63 – 16.67	26.16 *Wh*	0 *Wh*	26.16 *Wh*

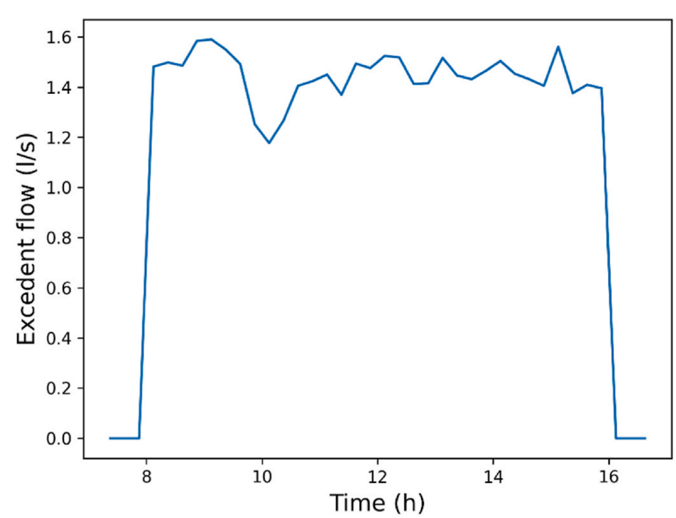

Fig. 12. Exceeding flows for the simulation period.

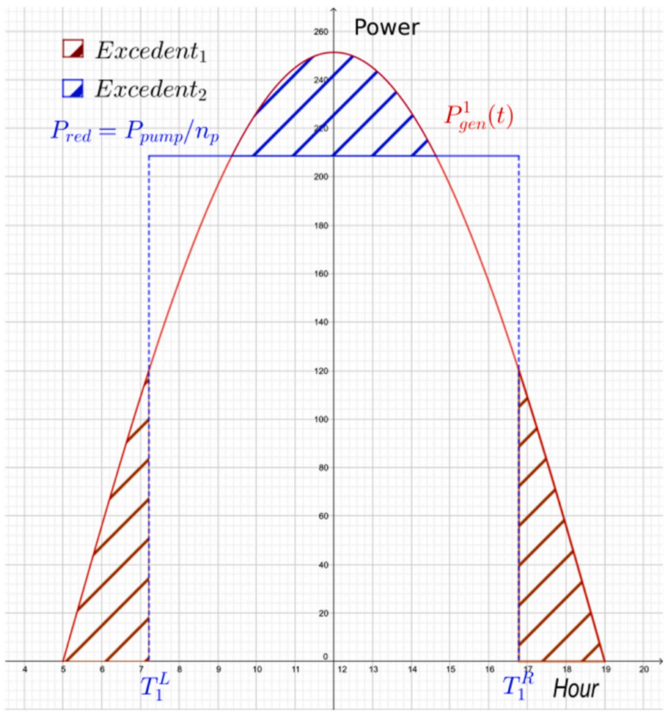

Fig. 13. Power generated and consumed for the July scenario with one pump in operation.

Table 2
Numerical results for the key variables corresponding to July.

Case I: One pump operating			
$T = \frac{V_{day}}{\lambda \bullet P_{red}}$	9.54 h	T^L_1 / T^R_1	7:13:39/16:46:21
Period	Energy stored	En. Consumed	Balance
4.75 – 7.22	87.31 *Wh*	0 *Wh*	87.31 *Wh*
7.22 – 9.82	392.89 *Wh*	542.69 *Wh*	– 149.80 *Wh*
9.82 – 14.18	1030.30 *Wh*	908.48 *Wh*	121.82 *Wh*
14.18 – 16.78	392.89 *Wh*	542.69 *Wh*	– 149.80 *Wh*
16.78 – 19.25	87.31 *Wh*	0 *Wh*	87.31 *Wh*

Analogously to December, we get equation (20) for July (and being $H(x)$ the Heaviside step function).

$$f_{July}(t) = P_{red,July} \bullet \left\{ H\left(T^R_{1,July}\right) - H\left(T^L_{1,July}\right) \right\}, \tag{20}$$

4. Discussion

Employing an off-grid system integrated with batteries offers a range of substantial advantages compared to an off-grid configuration devoid of battery storage. Batteries store energy from renewable sources like solar panels. This energy storage capacity ensures reliable power supply during low or varying renewable energy generation, reducing energy shortages and enhancing system reliability [27]. Additionally, batteries enable efficient load management, enabling users to optimise energy consumption patterns and reduce peak demand, leading to potential cost savings and reduced strain on the overall energy infrastructure. Batteries help off-grid systems adapt to sudden changes and unexpected events, making them more flexible and resilient.

This research builds on the authors' previous work and focuses on maximising energy use in isolated installations. To optimise the process, we look at every aspect of the problem, including solar panel installation and pump usage. Finally, the scheduling of irrigation in the PINs allows for optimising the performance obtained for each generated watt of energy in the system, minimising its waste. While there are studies on each problem individually, this paper offers a comprehensive analysis of them together.

The authors have researched improving irrigation system performance in different ways before. They have investigated the optimal sizing of solar panels to meet the energy demands of the pumps off-grid (Navarro-González et al., 2023). However, this approach did not account for batteries as a storage component. Previously, 435 panels were needed for this setup in December. Now, only 40 panels and a battery with a maximum storage capacity of 157 Wh (adjusted for safety to 240 Wh, 220V, and 70000mAh) are required. This method yields a reduction of 395 panels while ensuring minimal utilisation of a battery energy storage system. In July, the abundance of high irradiance results in increased energy generation. Even though water use doubled from December, we only need 16 solar panels and a battery with a 149.8 Wh storage capacity thanks to good system management. Consequently, Electricity generation has a bigger impact than water and energy consumption in this setup. Solar production is the more limiting factor, according to Ref. [19]. The system accommodates the entire year, entailing the installation of 40 panels (as derived from the December simulation). The University has excess energy in July that can be consumed or shared with the power grid.

Some other approaches used an economical approach to find the best choice, finding that PV/diesel/battery was the best option [43]. Batteries must be the right size for managing power in a microgrid during disruptions [44], and microgrid design and sizing are important to maintain stability during internal disturbances. In our approach, we have proposed the battery solution for a problem with peak power of 3.4 KW (with one pump) or 6.8 KW (with two pumps), values higher than 3 kW, the threshold in other works such as [8,9].

Batteries serve as energy reservoirs in photovoltaic systems [45], and a study explored the influence of PV technology on battery sizing for irrigation systems [46]. The findings underscored a noteworthy correlation between PV technology and the maximum stored energy capacity of the battery. Small differences in panel efficiency because of weather can change energy flow from pumping to battery storage.

Grid-connected and system-integrated solutions will lead the way in meeting future energy needs [47]. The advantages of such grid-connected solutions are manifold. They improve the stability and reliability of the power supply by seamlessly incorporating renewable energy sources into the grid. This can lead to a reduction in greenhouse gas emissions and a more sustainable energy mix [48,49]. Additionally, grid-connected photovoltaic systems enable the bi-directional flow of electricity, facilitating the storage of excess energy and its subsequent injection into the grid during periods of high demand or when the sun is not shining [50]. This optimises energy use in water networks and economic benefits both consumers (lower values for the cost of electricity as 0.18 US$/kWh [51]) and utility companies.

Future research in photovoltaic energy production for irrigation, combined with batteries, offers exciting possibilities. One important area is improving battery technology to enhance storage capacity and efficiency, maximising surplus energy from solar systems. Exploring new battery materials and designs could lead to more sustainable and reliable energy storage solutions. Another avenue is combining energy storage with other renewables like wind creating hybrid systems for consistent and resilient irrigation energy. Research in this area could offer adaptable solutions for diverse agricultural needs. Investigating the economic viability and scalability of photovoltaic energy with battery storage is crucial. Analysing costs, potential subsidies, and long-term financial sustainability can guide policies and adoption. The research could transform agriculture by providing reliable and eco-friendly energy solutions, which would benefit food security and environmental conservation.

Furthermore, we will explore critical aspects, such as assessing the effects of irradiance curves under different climatic conditions. Additionally, the challenge of optimising energy efficiency while considering energy supply prices in grid-connected facilities will be addressed. These approaches are essential for advancing the management and optimal use of renewable energy in an ever-changing environment.

5. Conclusions

This research optimises solar array size and backup battery used to maximise energy. The pumps are required to operate at maximum efficiency. After solving previous issues, we can focus on scheduling the irrigation plan that fits the pumping system's flow.

First, we proposed an optimisation algorithm for scheduling water delivery to crops. The energy management strategy's primary goal is to minimise energy surplus during each time interval. It achieves this by reducing the disparity between the energy produced (by the solar photovoltaic panels) and the energy consumed (by the pumping equipment used for crop irrigation). We adjust the pumping equipment and valve controls to match the new irrigation schedule.

This leads to adjustments in the operating points of the pumping equipment (start and stop times) and the automatic control of valve opening and closing times to align with the new irrigation schedule. Consequently, the cumulative demands arising from the irrigation valve openings result in a total flow and, overall energy supplied by the pumping system.

Furthermore, by adhering to the suggested algorithm, the energy consumed by the pumps and the energy input or storage in the batteries is meticulously aligned with the energy generated by the solar photovoltaic modules. This method satisfies water needs and reduces the number of solar panels and battery size. To achieve this, a sum of squared error minimisation objective function has been introduced to assess the discrepancies between the desired flow rate and the actual flow rate injected into the system. This facilitates the optimisation of the entire energy management process, leading to an efficient and well-balanced irrigation system.

Lastly, the algorithm efficiently returns as an output the irrigation scheduled plan to consume the highest energy available by solar PV modules.

This method has been tested in the actual PIN in San Vicente Campus, the University of Alicante, Spain (while applying to any other location). Currently, this network can work seven days a week with less energy consumption and is based only on solar PV energy. The new algorithm can save a lot of energy and reduce CO_2 emissions, leading to economic and environmental benefits.

We saved 90 % of solar panels and used a minimal battery energy storage system in the current method compared to the first study. In contrast, without batteries, off-grid systems are unstable and vulnerable to energy imbalances and supply disruptions. Thus, integrating batteries into an off-grid framework is a pivotal advancement that amplifies sustainability, reliability, adaptability, and efficiency.

Ethical approval and consent to participate

Not applicable.

Consent to publish

Not applicable.

CRediT authorship contribution statement

M.A. Pardo: Conceptualization, Methodology, Formal analysis, Data curation, analysis of results, Writing – review & editing. **F.J. Navarro-González:** Study conception and design, Methodology, Software, Formal analysis, Writing – review & editing.

Declaration of competing interest

The authors declare that they have no known competing financial interests or personal relationships that could have appeared to influence the work reported in this paper.

1 Acknowledgements

The authors have no conflicts of interest to declare. This work was supported by the project "*Hi-Edu Carbon*" "Erasmus Plus Programme, Key Action KA22021", action type (2021-1-SK01-KA220-HED-000023274).

7. Nomenclature

A Parameter of the Kasten-Czeplak model (Eq. (4))
B Parameter of the Kasten-Czeplak model (Eq. 4)
E_1^{gen} (Wh) daily energy generated by a single panel
$E_{panel}^1(\tau_1, \tau_2)$ (Wh) the energy generated by a single panel between the instants τ_1 and τ_2
$F_{n_p}^{-1}$ a function used to invert the relationship flow vs power
$F_1(Q_{max})$ (Wh) power consumed when one pump is delivering the maximum flow
$H(x)$ Heaviside step function
n_s (−) number of solar modules
n_s^* (−) minimum number of solar panels required to meet the needs
n_p (−) number of pumps in operation
P_0 (W/m^2) direct irradiance on a ground-level panel
P_{0N} (W/m^2) irradiance on a normal surface
$P_{gen}^1(t)$ (W) Power generated by a generic panel
$P_{gen}^{n_s}(t)$ (W) Power generated by using n_s panels
$P_{saved}(t)$ (W) Power stored in batteries
$\left(\frac{p}{\gamma}\right)_{th}$ (m.w.c.) Threshold pressure
$Q(t_k)$ available flow at t_k
Q_{max} Maximum flow that can be delivered
t (h) hour of the day
t_k (h) time
t_w (h) an arbitrary change in time
T (−) the greatest value for the index w

T_i^L (hour) starting operation time for the *i* pump
T_i^R (hour) stop operation time for the *i* pump
ω (−) the solar hour angle
x_1^c the intersection between the reduced power curve and energy consumption of *1* pump
V_{tot} (m^3) water demanded by crops

Greek Symbols

δ (−) the solar declination
δ_j^L (h) start time for *j* pump
δ_j^R (h) stop time for *j* pump
$\gamma(N/m^3)$ the specific weight of water
φ (−) Latitude
$\boldsymbol{\pi}$ (t_k) flow assigned at slice k
$\pi'(t_w)$ flow assigned at an arbitrary slice w considering a change in it
π_i (−) optimal operating power obtained from F_i
η_i (−) the i-th pump efficiency
τ_i (h) Generic *i* instant of time
θ_s (−) the solar zenith angle
$\Phi(\Pi)$ (−) objective function
Λ (−) maximum value of the difference $Q(t_i) - \pi(t_i)$

Acronyms

EU European Union
FAO Food and Agriculture Organization of the united nations
GHG greenhouse gas emissions
PIN pressurized irrigation network
PV photovoltaic

References

[1] S. Siebert, J. Burke, J.-M. Faures, K. Frenken, J. Hoogeveen, P. Döll, F.T. Portmann, Groundwater use for irrigation–a global inventory, Hydrol. Earth Syst. Sci. 14 (2010) 1863–1880.

[2] Y. Wada, L.P.H. Van Beek, M.F.P. Bierkens, Nonsustainable groundwater sustaining irrigation: a global assessment, Water Resour. Res. 48 (2012).

[3] FAO, The State of the World's Land and Water Resources for Food and Agriculture 2021 – Systems at Breaking Point, FAO, 2022, https://doi.org/10.4060/cb9910en.

[4] E. Commission, D.-G. for R. and Innovation, European Green Deal : Research & Innovation Call, Publications Office of the European Union, 2021, https://doi.org/10.2777/33415.

[5] W.P. Pauw, R.J.T. Klein, K. Mbeva, A. Dzebo, D. Cassanmagnago, A. Rudloff, Beyond headline mitigation numbers: we need more transparent and comparable NDCs to achieve the Paris Agreement on climate change, Clim. Change 147 (2018) 23–29, https://doi.org/10.1007/s10584-017-2122-x.

[6] R. Lacal Arantegui, A. Jäger-Waldau, Photovoltaics and wind status in the European union after the Paris agreement, Renew. Sustain. Energy Rev. 81 (2018) 2460–2471, https://doi.org/10.1016/j.rser.2017.06.052.

[7] INE, IPC-IPCA-Diciembre 2022 (2/14), Notas de Prensa, 2023, pp. 1–14. https://www.ine.es/daco/daco42/daco421/ipc1222.pdf. (Accessed 7 February 2023).

[8] Y. Yu, J. Liu, Y. Wang, C. Xiang, J. Zhou, Practicality of using solar energy for cassava irrigation in the Guangxi Autonomous Region, China, Appl. Energy 230 (2018), https://doi.org/10.1016/j.apenergy.2018.08.060.

[9] A. Parvaresh Rizi, A. Ashrafzadeh, A. Ramezani, A financial comparative study of solar and regular irrigation pumps: case studies in eastern and southern Iran, Renew. Energy 138 (2019), https://doi.org/10.1016/j.renene.2019.02.026.

[10] S. Rehman, I. El-Amin, Performance evaluation of an off-grid photovoltaic system in Saudi Arabia, Energy 46 (2012) 451–458, https://doi.org/10.1016/j.energy.2012.08.004.

[11] F.J. Navarro-Gonzalez, Y. Villacampa, M.Á. Pardo Picazo, M. Cortés-Molina, Optimal load scheduling for off-grid photovoltaic installations with fixed energy requirements and intrinsic constraints, Process Saf. Environ. Protect. 149 (2021) 476–484, https://doi.org/10.1016/j.psep.2020.11.011.

[12] Y. Tsuchiya, T.A. Swai, F. Goto, Energy payback time analysis and return on investment of off-grid photovoltaic systems in rural areas of Tanzania, Sustain. Energy Technol. Assessments 42 (2020), https://doi.org/10.1016/j.seta.2020.100887.

[13] D.H. Muhsen, A.B. Ghazali, T. Khatib, I.A. Abed, E.M. Natsheh, Sizing of a standalone photovoltaic water pumping system using a multi-objective evolutionary algorithm, Energy 109 (2016) 961–973, https://doi.org/10.1016/j.energy.2016.05.070.

[14] V. Zavala, R. López-Luque, J. Reca, J. Martínez, M.T. Lao, Optimal management of a multisector standalone direct pumping photovoltaic irrigation system, Appl. Energy 260 (2020), https://doi.org/10.1016/j.apenergy.2019.114261.

[15] M.Á. Pardo, R. Cobacho, L. Bañón, Standalone photovoltaic direct pumping in urban water pressurized networks with energy storage in tanks or batteries, Sustainability (2020) 12, https://doi.org/10.3390/su12020738.

[16] J. Farfan, C. Breyer, Combining floating solar photovoltaic power plants and hydropower reservoirs: a virtual battery of great global potential, in: Energy Procedia, Elsevier Ltd, 2018, pp. 403–411, https://doi.org/10.1016/j.egypro.2018.11.038.

[17] H. Rezk, A comprehensive sizing methodology for stand-alone battery-less photovoltaic water pumping system under the Egyptian climate, Cogent Eng 3 (2016), https://doi.org/10.1080/23311916.2016.1242110.

[18] S. Biswas, M.T. Iqbal, Dynamic modelling of a solar water pumping system with energy storage, Journal of Solar Energy 2018 (2018) 1–12, https://doi.org/10.1155/2018/8471715.

[19] M.Á. Pardo, H. Fernández, A. Jodar-Abellan, Converting a water pressurized network in a small town into a solar power water system, Energies 13 (2020), https://doi.org/10.3390/en13154013.

[20] T. Novosel, B. Ćosić, T. Pukšec, G. Krajačić, N. Duić, B.V. Mathiesen, H. Lund, M. Mustafa, Integration of renewables and reverse osmosis desalination – case study for the Jordanian energy system with a high share of wind and photovoltaics, Energy 92 (2015) 270–278, https://doi.org/10.1016/J.ENERGY.2015.06.057.

[21] P. Cabrera, H. Lund, J.A. Carta, Smart renewable energy penetration strategies on islands: the case of Gran Canaria, Energy 162 (2018) 421–443, https://doi.org/10.1016/J.ENERGY.2018.08.020.

[22] S.S. Torbaghan, N. Blaauwbroek, D. Kuiken, M. Gibescu, M. Hajighasemi, P. Nguyen, G.J.M. Smit, M. Roggenkamp, J. Hurink, A market-based framework for demand side flexibility scheduling and dispatching, Sustainable Energy, Grids and Networks 14 (2018) 47–61, https://doi.org/10.1016/J.SEGAN.2018.03.003.

[23] P.A. Østergaard, H. Lund, B.V. Mathiesen, Energy system impacts of desalination in Jordan, International Journal of Sustainable Energy Planning and Management 1 (2014) 29–40.

[24] A.M. Delgado-Torres, L. García-Rodríguez, Off-grid SeaWater Reverse Osmosis (SWRO) desalination driven by hybrid tidal range/solar PV systems: sensitivity analysis and criteria for preliminary design, Sustain. Energy Technol. Assessments 53 (2022), https://doi.org/10.1016/j.seta.2022.102425.

[25] W. He, G. Huang, C.N. Markides, Synergies and potential of hybrid solar photovoltaic-thermal desalination technologies, Desalination 552 (2023), https://doi.org/10.1016/j.desal.2023.116424.

[26] K. Liu, B. Sun, X. Gao, Y. Zhang, W. Sun, Q. Feng, W. Yang, Optimal sizing of the stand-alone photovoltaic system for a solar-powered translational sprinkler irrigation machine considering the loss of power supply probability, Math. Probl Eng. 2022 (2022), https://doi.org/10.1155/2022/6133969.

[27] M.Á. Pardo, J. Manzano, J. Valdes-Abellan, R. Cobacho, Standalone direct pumping photovoltaic system or energy storage in batteries for supplying irrigation networks. Cost analysis, Sci. Total Environ. 673 (2019) 821–830, https://doi.org/10.1016/j.scitotenv.2019.04.050.

[28] F.J. Navarro-González, M.Á. Pardo, H.E. Chabour, T. Alskaif, An irrigation scheduling algorithm for sustainable energy consumption in pressurised irrigation networks supplied by photovoltaic modules, Clean Technol. Environ. Policy (2023), https://doi.org/10.1007/s10098-023-02486-3.
[29] J.M. Carricondo-Antón, M.A. Jiménez-Bello, J. Manzano Juárez, A. Royuela Tomas, A. Sala, Evaluating the use of meteorological predictions in directly pumped irrigational operations using photovoltaic energy, Agric. Water Manag. 266 (2022), https://doi.org/10.1016/j.agwat.2022.107596.
[30] N. Mousavi, G. Kothapalli, D. Habibi, C.K. Das, A. Baniasadi, A novel photovoltaic-pumped hydro storage microgrid applicable to rural areas, Appl. Energy 262 (2020), https://doi.org/10.1016/j.apenergy.2019.114284.
[31] A. Mérida García, I. Fernández García, E. Camacho Poyato, P. Montesinos Barrios, J.A. Rodríguez Díaz, Coupling irrigation scheduling with solar energy production in a smart irrigation management system, J. Clean. Prod. 175 (2018) 670–682, https://doi.org/10.1016/j.jclepro.2017.12.093.
[32] T. AlSkaif, A.C. Luna, M.G. Zapata, J.M. Guerrero, B. Bellalta, Reputation-based joint scheduling of households appliances and storage in a microgrid with a shared battery, Energy Build. 138 (2017) 228–239, https://doi.org/10.1016/j.enbuild.2016.12.050.
[33] G. Zubi, R. Dufo-López, M. Carvalho, G. Pasaoglu, The lithium-ion battery: state of the art and future perspectives, Renew. Sustain. Energy Rev. 89 (2018), https://doi.org/10.1016/j.rser.2018.03.002.
[34] T. Terlouw, T. AlSkaif, C. Bauer, W. van Sark, Multi-objective optimization of energy arbitrage in community energy storage systems using different battery technologies, Appl. Energy 239 (2019) 356–372, https://doi.org/10.1016/j.apenergy.2019.01.227.
[35] H.C. Hesse, M. Schimpe, D. Kucevic, A. Jossen, Lithium-ion battery storage for the grid - a review of stationary battery storage system design tailored for applications in modern power grids, Energies 10 (2017), https://doi.org/10.3390/en10122107.
[36] M.M. Symeonidou, C. Zioga, A.M. Papadopoulos, Life cycle cost optimization analysis of battery storage system for residential photovoltaic panels, J. Clean. Prod. 309 (2021), https://doi.org/10.1016/j.jclepro.2021.127234.
[37] H. Rezk, M.A. Abdelkareem, C. Ghenai, Performance evaluation and optimal design of stand-alone solar PV-battery system for irrigation in isolated regions: a case study in Al Minya (Egypt), Sustain. Energy Technol. Assessments 36 (2019), https://doi.org/10.1016/j.seta.2019.100556.
[38] P. Ineichen, Validation of models that estimate the clear sky global and beam solar irradiance, Sol. Energy 132 (2016) 332–344, https://doi.org/10.1016/j.solener.2016.03.017.
[39] Z.K. Pecenak, F.A. Mejia, B. Kurtz, A. Evan, J. Kleissl, Simulating irradiance enhancement dependence on cloud optical depth and solar zenith angle, Sol. Energy 136 (2016) 675–681, https://doi.org/10.1016/j.solener.2016.07.045.
[40] M. Järvelä, K. Lappalainen, S. Valkealahti, Characteristics of the cloud enhancement phenomenon and PV power plants, Sol. Energy 196 (2020) 137–145, https://doi.org/10.1016/j.solener.2019.11.090.
[41] J.A. Duffie, W.A. Beckman, Solar Engineering of Thermal Processes, John Wiley & Sons, 2013.
[42] M.A. Pardo, F.J. Navarro-González, Y. Villacampa, An algorithm to schedule water delivery in pressurized irrigation networks, Comput. Electron. Agric. 201 (2022), https://doi.org/10.1016/j.compag.2022.107290.
[43] M.Z. Abid, M. Yousif, S. Ullah, M. Hassan, Design, sizing and economic feasibility of a hybrid PV/diesel/battery based water pumping system for farmland, Int. J. Green Energy 19 (2022) 614–637, https://doi.org/10.1080/15435075.2021.1954007.
[44] M. Abdel-Salam, A. Ahmed, H. Ziedan, R. Kamel, K. Sayed, M. Amery, M. Swify, Steady-state modeling and control of a microgrid supplying irrigation load in Toshka Area, in: IECON Proceedings (Industrial Electronics Conference), 2012, https://doi.org/10.1109/IECON.2012.6389056.
[45] M.E. Glavin, W.G. Hurley, Optimisation of a photovoltaic battery ultracapacitor hybrid energy storage system, Sol. Energy 86 (2012) 3009–3020, https://doi.org/10.1016/j.solener.2012.07.005.
[46] L. Stoyanov, I. Bachev, Z. Zarkov, V. Lazarov, Study of PV technology influence on the battery sizing in PV-based irrigation system, in: 2022 8th International Conference on Energy Efficiency and Agricultural Engineering, EE and AE 2022 - Proceedings, Institute of Electrical and Electronics Engineers Inc., 2022, https://doi.org/10.1109/EEAE53789.2022.9831337.
[47] M. Morey, N. Gupta, M.M. Garg, A. Kumar, A comprehensive review of grid-connected solar photovoltaic system: architecture, control, and ancillary services, Renewable Energy Focus 45 (2023) 307–330, https://doi.org/10.1016/j.ref.2023.04.009.
[48] K.N. Nwaigwe, P. Mutabilwa, E. Dintwa, An overview of solar power (PV systems) integration into electricity grids, Mater Sci Energy Technol 2 (2019), https://doi.org/10.1016/j.mset.2019.07.002.
[49] M. Shafiullah, S.D. Ahmed, F.A. Al-Sulaiman, Grid integration challenges and solution strategies for solar PV systems: a review, IEEE Access 10 (2022), https://doi.org/10.1109/ACCESS.2022.3174555.
[50] C. Roselli, G. Diglio, M. Sasso, F. Tariello, A novel energy index to assess the impact of a solar PV-based ground source heat pump on the power grid, Renew. Energy 143 (2019), https://doi.org/10.1016/j.renene.2019.05.023.
[51] O.C. Akinsipe, D. Moya, P. Kaparaju, Design and economic analysis of off-grid solar PV system in Jos-Nigeria, J. Clean. Prod. 287 (2021), https://doi.org/10.1016/j.jclepro.2020.125055.